Preprint typeset using LaTeX style emulateapj v. 10/09/06

THE ONCE AND FUTURE ANDROMEDA STREAM

Masao Mori[1]
Department of Law, Senshu University, Higashimita 2-1-1, Tama, Kawasaki 214-8580, Japan
and
R. Michael Rich
Department of Physics and Astronomy, University of California, Los Angeles, CA 90095-1562, USA

ABSTRACT

The interaction between an accreting satellite and the Andromeda galaxy has been studied using an N-body simulation to investigate the self-gravitating response of the disk, the bulge, and the dark matter halo to an accreting satellite. Our simulation shows that the "giant stream" is the tidal debris of the infalling satellite. The debris also produces diffuse shells on the east and the west side of M31 in agreement with observations, but for an accreting satellite mass of $M \leq 5 \times 10^9 M_\odot$, the disk survives the collision in its present form and negligible disk stars are ejected into the halo. Following the evolution of the merger past the present day, these shells expand further and a multiple large scale-shell system is finally formed in the outer region and a dense core forms in the inner region. The outermost large-scale shells in our simulation have a radius of > 50 kpc and these structures survive at least 4 Gyr from the present-day. We propose that recently discovered distant arc-like structures and metal rich stars at $R > 100$ kpc may be the remnants of ancient radial infall collisions similar to the one responsible for the currently observed giant stream.

Subject headings: galaxies: interactions — galaxies: kinematics and dynamics — galaxies: individual (M31)

1. INTRODUCTION

Large spiral galaxies like the Andromeda galaxy (M31) are believed to have formed in part from the merger of many less massive galaxies, and their halos are modeled as the debris of accreted dwarfs (e.g. Bullock & Johnston 2005). The giant stream of Ibata et al. (2001) and the starcount maps of Ferguson et al. (2002) establish the complex merger origin of the M31 halo population; evidence for coherent structures now extends to ≈ 100 kpc (Ibata et al. 2007). Further support comes from the spectroscopic side e.g. the disk population of Ibata et al. (2005). Deep photometry with the *HST* shows that three deep fields in the M31 halo exhibit unequivocal evidence for intermediate age populations (Brown et al. 2006). Starcount maps and radial velocities of red giant stars near M31 exhibit a giant stellar stream to the south of this galaxy, as well as giant stellar shells to the east and the west of M31's center (Ibata et al. 2001; Ferguson et al. 2002; McConnachie et al. 2003; Ibata et al. 2004; Ibata et al. 2005; Guhathakurta et al. 2006). The giant southern stream has a projected length of ~ 60 kpc and a physical length of ~ 120 kpc from its tip south and behind M31 into M31's center. There is further a shell-like overdensity at the east (west) side at $\xi \sim 1.8°, \eta \sim 0.7°$ ($\xi \sim -1.5°, \eta \sim 0.7°$).

N-body simulations suggest that these structures are the tidal debris formed in the last pericentric passage of a satellite on a radial orbit (Ibata et al. 2004; Font et al. 2006; Geehan et al. 2006; Fardal et al. 2006, 2007). However, these models of the interaction between the progenitor of the giant stream and M31 have always assumed a fixed potential to represent the influence of M31 (Ibata et al. 2004; Font et al 2006; Geehan et al 2006; Fardal et al 2006, 2007). The discovery of the widespread intermediate age halo population has raised the question of whether these stars belong to the infalling satellite or are instead disk stars that were ejected in the stream collision or an earlier interaction. We can answer this question only if our simulations include, in addition to the satellite, a live (N-body) disk and bulge.

In this Letter, to investigate the self-gravitating response of the disk, the bulge, and the dark matter halo to accreting satellite, we use a self-consistent N-body model of M31 derived from a composite distribution function by Widrow, Perrett & Suyu (2003) and the orbital parameters of Fardal et al. (2007).

2. M31 DISK THICKNESS CONSTRAINS THE SATELLITE MASS

The disk heating due to the infalling satellites is the important issue in terms of the observed disk thickness of disk galaxies (Tóth & Ostriker 1992; Quinn, Hernquist & Fullagar 1993; Velázquez & White 1999; Font et al. 2001; Hayashi & Chiba 2006; Gauthier, Dubinski & Widrow 2006). This section addresses the effect of the stream progenitor on the disk thickness; the observed thickness of M31's disk provides a possible limit on the mass of the progenitor.

We estimate the disk heating by dynamical friction which is caused by the scattering of the disk stars into an overdense wake that trails the orbiting body and tugs back on the scatter. The energy input into disk stars getting through the interaction between disk stars and a satellite is equal to the orbital energy loss ΔE of the satellite. If we assume that the vertical velocity dispersion of the disk stars σ_z is constant, the change $\Delta\sigma_z$ is simply denoted by $\Delta\sigma_z^2 = 2\Delta E/M_s$, where M_s is the

Electronic address: mmori@isc.senshu-u.ac.jp
Electronic address: rmr@astro.ucla.edu
[1] Visiting researcher of Department of Physics and Astronomy, University of California, Los Angeles

mass of the satellite, and ΔE is given by the integral of a frictional force over an orbit of a satellite within a disk. Using the Chandrasekhar formula of the dynamical friction (Chandrasekhar 1943) for a thin disk, ΔE is roughly estimated by $\Delta E \simeq 4\pi\ G^2 M_{\rm s}^2 \Sigma / v_{\rm s}^2$, where G is the gravitational constant, Σ is the surface mass density of a disk and $v_{\rm s}$ is the satellite velocity.

For an axisymetric thin disk, the equation of motion in the vertical direction and the Poisson equation are simply expressed by $\partial_{\rm z}(\rho_{\rm d}\sigma_{\rm z}^2) + \rho_{\rm d}\partial_{\rm z}\Phi = 0$ and $\partial_{\rm z}^2\Phi = 4\pi G\rho_{\rm d}$, where $\rho_{\rm d}$ is the mass density of the disk and Φ is the gravitational potential, respectively. Using these equations and assuming the $\rho_{\rm d} \propto \exp(-z/z_{\rm d})$, where $z_{\rm d}$ is the scale hight of the disk, we obtain the relation between $\sigma_{\rm z}$ and $z_{\rm d}$ such as $\sigma_{\rm z}^2 = 2\pi G\Sigma z_{\rm d}$. Inserting the equation of $\Delta\sigma_{\rm s}^2$ into the change of the vertical velocity dispersion of the disk as $\Delta\sigma_{\rm z}^2 = 2\pi G\Sigma\Delta z_{\rm d}$, we get the relation as $\Delta z_{\rm d} = 4GM_{\rm s}^2/(M_{\rm d}v_{\rm s}^2)$.

Using the virial velocity $v_{\rm s} = GM_{\rm v}/R_{\rm v} = 150$ km s^{-1}, where $M_{\rm v}(= 4.2 \times 10^{11}\ M_\odot)$ is the virial mass and $R_{\rm v}(= 80$ kpc) is the virial radius, and the observed disk thickness of M31, $\Delta z_{\rm d} = 0.3$ kpc (Kuijken & Dubinski 1995), finally, we obtain the critical satellite mass,

$$M_{\rm c} = 5.2 \times 10^9 M_\odot \times \left(\frac{M_{\rm d}}{7\times10^{10}\ M_\odot}\right)^{1/2} \left(\frac{v_{\rm s}}{150\ {\rm km\ s^{-1}}}\right) \left(\frac{\Delta z_{\rm d}}{0.3\ {\rm kpc}}\right)^{1/2} \quad (1)$$

Consequently, the dynamical mass of the satellite should be smaller than this critical mass since the disk thickness must agree with the observed thickness of M31 after the interaction of the satellite. *This yields an upper limit for the total progenitor mass.* Adopting for the stream [Fe/H]$\gtrsim -1$ (Koch et al. 2007) and using the mass-metallicity relation of Dekel & Woo (2003) implies a lower mass limit for a progenitor stellar mass $\approx 5 \times 10^8 M_\odot$ which agrees with the predictions of Font et al. (2006, 2007).

3. NUMERICAL MODELING OF THE INTERACTION BETWEEN THE SATELLITE AND M31

The discussion in the previous section is an order of magnitude, and therefore, detailed structure and evolution of the system should be verified by fully nonlinear and time dependent numerical simulations.

We assume that the total mass of the disk is $7.0 \times 10^{10} M_\odot$. The density of the disk falls off approximately as the exponential with the scale length of 5.4 kpc in the radial direction, and as sech^2 with the scale height of 0.3 kpc in the vertical direction. The bulge is a King (1966) model with total mass of $2.5 \times 10^{10} M_\odot$. The dark matter halo is taken to be a lowered Evans model (Kuijken & Dubinski 1995) with the total mass of $3.2 \times 10^{11} M_\odot$ and the tidal radius of 80 kpc. This set of parameters corresponds to the Model A of Widrow, Perrett & Suyu (2003), and provides a good match with the observational data for M31. An N-body realization of this model is done by GalactICS code written by Kuijken & Dubinski (1995). The satellite is assumed to be a Plummer sphere with the initial mass of $10^9 M_\odot$ (Model A), $5 \times 10^9 M_\odot$ (Model B) and $10^{10} M_\odot$ (Model C). The initial scale radius is 1 kpc. Following Fardal et al. (2007), we adopt the initial position vector and velocity vector for the standard coordinates centered from M31 are (-34.75, 19.37, -13.99) kpc and (67.34, -26.12, 13.50) km s^{-1} , respectively. The evolution of a collisionless system is followed up to 5 Gyr using the parallel N-body code, Gadget-2 written by Springel (2005). We adopt a tree algorithm with a tolerance parameter of $\theta = 0.5$ and a softening length is 50 pc for all particles. The number of particles is 7,351,266 for the disk, 2,581,897 for the bulge, and 30,750,488 for the dark matter halo. For the satellite, we use 10^5 particles for Model A, 5×10^5 particles for Model B, and 10^6 particles for Model C. The total number of particles is about 40 million and the a particle mass is $\sim 10^4 M_\odot$.

Figure 1a-1h shows the results for the time sequence of stellar dynamics for Model A. The upper panels in double columns illustrate the spatial distribution of stellar density as a function of time from -1 to -0.25 Gyr (where 0 Gyr is present day). The lower panels describe the *future* evolution of the system from the present-day to 3 Gyr. In our time frame, -1 Gyr corresponds to the initial condition and the start of the simulation run. The first pericentric passage from the start of simulation occurred about 0.7 Gyr ago. Figure 1b shows that the satellite collides almost head-on with the bulge. Then, the distribution of satellite particles is distorted and is spread out significantly as seen in Fig. 1c. A large fraction of the satellite particles acquire a high velocity relative to the center of M31. This debris expands at great distance, keeping a narrow distribution and it gives rise to the southern giant stream. The apocentric passage has been seen about 0.5 Gyr ago and the second pericentric passage has been observed in Fig. 1c. As seen in Fig. 1d, stellar particles that initially constituted the satellite start to form a clear shell structure after the second collision with the disk. Moreover, a double shell system is sharply defined in Fig. 1e. The system is composed of approximately constant curvature shells formed by phase wrapping. Then, these shells further expand and a multiple large scale-shell system is finally formed in the outer region and the dense core is formed in the inner region. The outermost large-scale shells in our simulation have a radius of > 50 kpc and these structures survive at least 4 Gyr from the present-day.

Figure 2 shows the comparison between the map of RGB count density around M31 observed by Irwin et al. (2005) and the projected stellar density at the present-day. The satellite is entirely torn apart and the giant stream of debris which caused tidal destruction of the accreting satellite at the southern part of M31 is observed. The total mass of the stream given by simulation is $1.4 \times 10^8 M_\odot$. This is consistent with the estimated mass $\sim 3 \times 10^8 M_\odot$ from the observations by Ibata et al (2001). Furthermore, butterfly-shaped shells are formed in the northeast and the west part of M31. In the RGB count map of Irwin et al. (2005), the brightness of the northeast shell appears to exceed that of the west shell. The observed density contrast between the shells is 0.43 at $(\xi, \eta) = (2.0, 0.7)$ and (-1.5, 0.7) with the radius of 0.5 deg for the standard coordinates centered from M31. On the other hand, our modeled density contrast is 0.25. While this is lower than is observed, our simulated debris reasonably matches the observed faint features in M31.

Figure 3 shows the disk thickness $< z >^{1/2}$ as a function of the radius following the interaction for the different satellite models. The solid line and the dashed line

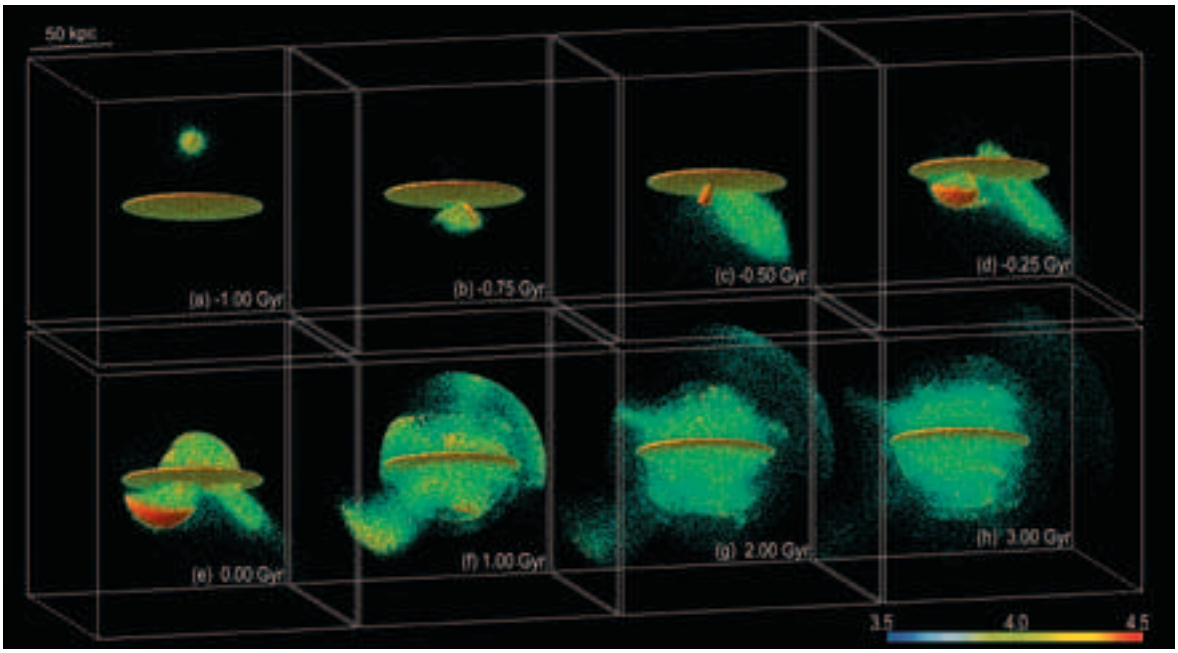

FIG. 1.— Morphological evolution of the satellite. (a)-(f) The spatial distribution of stellar density as a function of the elapsed time, where 0.00 Gyr corresponds to the present. Elapsed time in Gyr is given at the lower-right corner of the left panels: (a)-1.00 Gyr, (b)-0.75 Gyr, (c)-0.50 Gyr, (d)-0.25 Gyr, (e) 0.0 Gyr, (f) 1.0 Gyr, (g) 2.0 Gyr, and (h) 3.0 Gyr, respectively. Notice the formation of shells in 1(e): distant arcs observed by Ibata et al. (2007) may correspond to the shells of an ancient radial merger. This figure is also available as an mpeg animation in *http://www.isc.senshu-u.ac.jp/∼thj0613/M31/M31.html*.

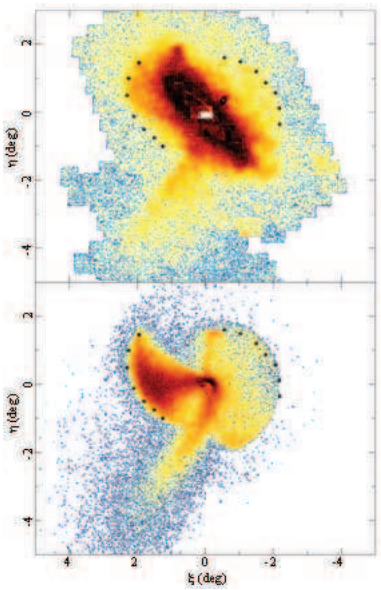

FIG. 2.— Comparison between our simulation and the observed star counts. *Upper*: The map of RGB count density around M31 observed by Irwin et al. (2005). *Lower*: The projected stellar density of Model A.

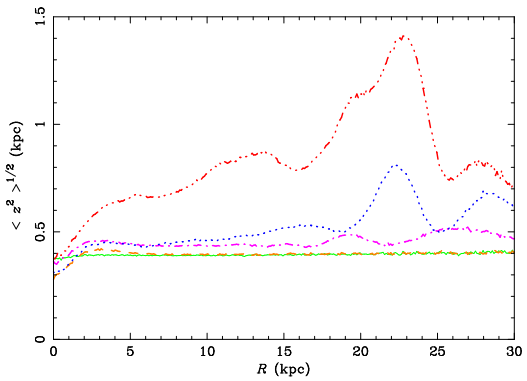

FIG. 3.— Vertical extent of the disk at the present-day for different impact satellite masses. The solid line and the dshed line show the initial radial profile and the resultant radial profile after 5 Gyr without a collision, respectively The dot-dashed line, the dotted line and the dot-dot-dot-dashed line correspond to Models A, B and C, ($10^9, 5\times10^9$, and $10^{10} M_\odot$) respectively. Notice that our preferred Modal A has a negligible effect on the disk.

show the initial radial profile and the resultant radial profile after 5 Gyr *without* the infalling satellite, respectively. A concordance of two lines confirms that our fiducial model of M31 has perfect dynamical stability during the integration time. There is no significant impact on the disk kinematics of the disk thickness for Model A and B. But it is clear that the massive satellite (Model C) is more effective for disk heating than the less massive satellites. For the inner part of the disk, $R < 10$ kpc, the scale height increases less than $\sim 10\%$ its initial value for Model A and B, and more than $\sim 50\%$ for Model C. Thus, a massive satellite is ruled out for the progenitor of the Andromeda giant stream and this result confirms the discussion given in §2.

4. DISCUSSION

In this work, we follow the approach of Fardal et al. (2007) in simulating the infall of a massive satellite into M31. However, we add a live N-body disk and bulge, and this permits us to ask under what conditions this collision might eject stars from these populations into the halo and quantifies the effect of these populations on the satellite. We also follow the evolution of this encounter for 4 Gyr beyond the present. As is the case in Fardal's work, our simulations successfully reproduce the

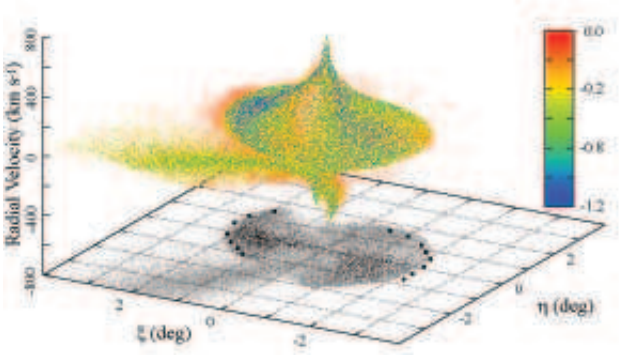

FIG. 4.— Phase space distribution of the satellite particles. The color of each particle corresponds to the initial total energy with the unit of 10^{51} erg, with more negative values having originally been deeper in the potential. Notice the preponderance of particles that were originally deep in the potential that are found in the East shell.

giant stream and apparent shell structures that are observed in the starcount maps. The large number of test particles in our satellite affords a good comparison with observations (Koch et al. 2007). We conclude that the event responsible for the giant stream most likely has not populated the halo with ejected disk stars; hence the intermediate age metal rich populations observed in deep HST fields by Brown et al. (2006) are not disk stars ejected *by the stream progenitor.* An ancient radial collision involving a more massive progenitor ($\approx 10^{10} M_{\odot}$), or a collision with a different approach angle, might have been capable of ejecting disk stars into the halo. The present day thickness of the disk following this collision constrains the progenitor mass to be $< 5 \times 10^{9} M_{\odot}$.

Our simulation gives some unexpected predictions, such as the existence of high velocity stars in the central region of M31. Figure 4 shows that the tidal debris in the M31 central bulge has velocity > 300 km s^{-1}. The particles that were originally deepest in the potential (see color-coding in 10^{51} erg units) are in the east shell.

Observations in this region might reveal additional clues about the nature of the satellite, such as the central metallicity. It is also noteworthy that > 3 Gyr after the collision, the debris more or less uniformly fills the halo. Simulations such as Font et al. (2007) may wish to consider the disk, bulge, halo, and satellite stellar populations and their effect on the long term evolution of streams; encounters with stars in the disk and bulge may disrupt the coherence of streams and scatter the stars in a manner analogous to disk and bulge shocking of globular clusters.

Recently Ibata et al. (2007) have carried out a deep, wide field photometric survey of the minor axis toward M33. They detect a series of arc-like structures which lie between M31 and M33. All of them are parallel to the major axis of M31 and the separation between arcs is ≈ 10 kpc (see Ibata et al. 2007). These faint structures are similar to the large-scale shell structures shown in Fig. 1f-1h. We conclude that these arcs may be the fossils of previous radial mergers several Gyr in the past. Our model predicts that similar arcs should be found on the opposite side of the M31 disk, in the Northwest quandrant, if in fact they are the shells of ancient radial infall collisions. Our model also offers a natural explanation for stars with $R > 100$ kpc that are observed in the M31 halo near the systemic velocity of M31 (Gilbert et al. 2006; Koch et al. 2007). Some of these stars at $R \approx 165$ kpc are found to have [Fe/H]$=-1$ by Koch et al. (2007). We propose that these stars are *not* a pressure supported halo but are rather the remnants of ancient radial collisions (note that in Fig. 1, the final extent of the collision is of order 100 kpc). Future studies will examine collisions from different attack angles, stellar disks, and the fate of dust and gas.

We are grateful to A. Koch, H. Ferguson, and D. Reitzel for valuable discussions. We thank M. J. Irwin for use of observational data, K. Shimasaku for data processing, and M. Umemura for use of the FIRST cluster. The computations were performed on the FIRST cluster at CCS, the University of Tsukuba and the SPACE at Senshu University. MM was supported in part by the Grant-in-Aid of the JSPS, 14740132, and by Grants-in-Aid of the MEXT, 16002003. RMR acknowledges support from GO-10265 and 10816 from the Space Telescope Science Institute, and grants AST-039731, and AST-0709479 from the National Science Foundation.

REFERENCES

Brown, T. M., Smith, E., Ferguson, H. C., Rich, R. M., Guhathakurta, P., Renzini, A., Sweigart, A. V., & Kimble, R. A. 2006, ApJ, 652, 323
Bullock, J. S., & Johnston, K. V. 2005, ApJ, 635, 931
Chandrasekhar, S. 1943, ApJ, 97, 255
Dekel, A. & Woo, J. 2003, MNRAS, 344, 1131
Fardal, M. A., Babul, A., Geehan, J. J., & Guhathakurta, P. 2006, MNRAS, 366, 1012
Fardal, M. A., Guhathakurta, P., Babul, A., & McConnachie, A. W. 2007, MNRAS, 380, 15
Ferguson, A. M. N., Irwin, M. J., Ibata, R. A., Lewis, G. F., & Tanvir, N. R., 2002, AJ, 124, 1452
Font, A. S., Navarro, J. F., Stadel, J., & Quinn, T. 2001, ApJ, 563, L1
Font, A. S., Johnston, R. A., Guhathakurta, P., Majewski, S. R., & Rich, R. M. 2006, AJ, 131, 1436
Font, A. S., Johnston, K. V., Ferguson, A. M. N., Bullock, J. S., Robertson, B. E., Tumlinson, J., & Guhathakurta, P. 2007, ArXiv e-prints, 709, arXiv:0709.2076
Gauthier, J.-R., Dubinski, J., & Widrow, L. M. 2006, ApJ, 653, 1180
Geehan, J. J., Fardal, M. A., Babul, A., & Guhathakurta, P. 2006, MNRAS, 366, 996
Guhathakurta, P., Rich, R. M., Reitzel, D. B., Cooper, M. C., Gilbert, K. M., Majewski, S. R., Ostheimer, J. C., Geha, M. C., Johnston, K. V., & Patterson, R. J. 2006, AJ, 131, 2497
Hayashi, H., & Chiba, M. 2006, PASJ, 58, 835
Ibata, R. A., Irwin, M. J., Ferguson, A. M. N., Lewis, G., & Tanvir, N. 2001, Nature, 412, 49
Ibata, R. A., Chapman, S., Ferguson, A. M. N., Irwin, M. J., Lewis, G., & McConnachie, A. 2004, MNRAS, 351, 117
Irwin, M. J., Ferguson, A. M. N., Ibata, R. A., Lewis, G. F., & Tanivir, N. R. 2005, ApJ, 628, L105
Ibata, R. A., Martin, N. F., Irwin, M., Chapman, S., Ferguson, A. M. N., Lewis, G. F., McConnachie, A. W. 2007/ astro-ph arXiv:0704.1318v1
King, I. R. 1966, AJ, 67, 471
Koch, A. et al. ApJ submitted.
Kuijken, K., & Dubinski, J. 1995, MNRAS, 277, 1341
McConnachie, A. W., Irwin, M. J., Ibata, R. A., Ferguson, A. M. N., Lewis, G. F., & Tanvir, N. 2003, MNRAS, 343, 1335
Quinn, P. J., Hernquist, L., & Fullagar, D. P. 1993, ApJ, 403, 74

Springel, V. 2005, MNRAS, 364, 1105
Tóth, G., & Ostriker, J. P. 1992, ApJ, 389, 5
Velázquez, H., & White, S. D. M. 1999, MNRAS, 304, 254
Widrow, L. M., Perrett, L. M. & Suyu, S. H. 2003, ApJ, 588, 311